Convergence of a cartesian method for elliptic problems with immersed interfaces

Lisl Weynans

Convergence of a cartesian method for elliptic problems with immersed interfaces

L. Weynans[1]

[1]**Team Memphis, INRIA Bordeaux-Sud-Ouest & CNRS UMR 5251, Université de Bordeaux, France**

RESEARCH REPORT

N° 8872

Septembre 2017

Project-Teams Memphis

ISSN 0249-6399 ISRN INRIA/RR--8872--FR+ENG

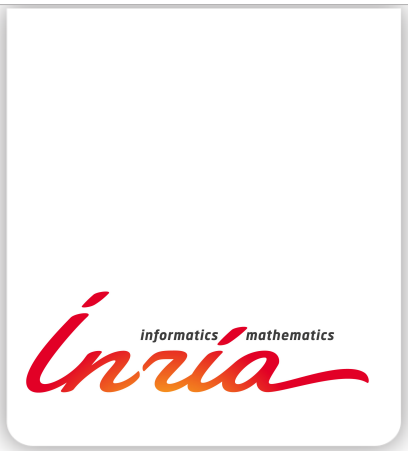

Convergence of a cartesian method for elliptic problems with immersed interfaces

L. Weynans[1]*

[1]Team Memphis, INRIA Bordeaux-Sud-Ouest & CNRS UMR 5251,
Université de Bordeaux, France

Project-Teams Memphis

Research Report n° 8872 — Septembre 2017 — 24 pages

Abstract:
We study in this paper the convergence of a Cartesian method for elliptic problems with immersed interfaces that was introduced in a previous paper [7]. This method is based on additional unknowns located on the interface, used to express the jump conditions across the interface and to discretize the elliptic operator in each subdomain separately. It is numerically second-order accurate in L^∞-norm. This paper is a step toward the convergence proof of this method. Indeed, we prove the convergence of the method in two cases: the original second-order method in one dimension, and a first-order version in two dimensions. The proof of convergence uses discrete Green's functions and takes advantage of a discrete maximum principle to obtain estimates on the coefficients of the inverse matrix.

Key-words: Finite-differences, cartesian method, elliptic problem, interface discontinuity, interface unknowns, discrete Green's function, convergence

* Corresponding author: lisl.weynans@inria.fr

RESEARCH CENTRE
BORDEAUX – SUD-OUEST

351, Cours de la Libération
Bâtiment A 29
33405 Talence Cedex

Convergence d'une méthode cartésienne pour des problèmes elliptiques avec interfaces immergées

Résumé : Nous étudions dans ce rapport la convergence d'une méthode sur grille cartésienne pour des problèmes elliptiques avec des interfaces immergées, introduite dans [7]. Cette méthode repose sur l'utilisation d'inconnues supplémentaires situées sur l'interface, qui servent à discrétiser séparément l'opérateur elliptique dans chaque sous-domaine et à exprimer avec une précision suffisante les conditions de saut au travers de l'interface. Il a été montré numériquement dans [7] que cette méthode converge à l'ordre deux en norme L^∞. Cet article est un pas en avant vers la preuve de la convergence de cette méthode. En effet, nous prouvons la convergence dans deux cas: celui de la méthode originale en une dimension, et celui d'une version à l'ordre un, mais en deux dimensions. La preuve de convergence fait appel à des fonctions de Green discrètes et tire profit d'un principe du maximum discret pour obtenir des estimations des coefficients de la matrice inverse.

Mots-clés : Différences finies, problème elliptique, méthode cartésienne, discontinuité au travers de l'interface, inconnues sur l'interface, fonction de Green discrète, convergence

Contents

1 Introduction

In this paper we aim to study the convergence of a method developed in a previous paper [7] to solve on a Cartesian grid the following problem elliptic problem, defined on a domain Ω consisting in the union of two subdomains Ω_1 and Ω_2, separated by a complex interface Σ (see Figure 1):

$$-\nabla.(k\nabla u) = f \text{ on } \Omega = \Omega_1 \cup \Omega_2 \tag{1}$$

$$[\![u]\!] = \alpha \text{ on } \Sigma \tag{2}$$

$$[\![k\frac{\partial u}{\partial n}]\!] = \beta \text{ on } \Sigma \tag{3}$$

with k constant on each subdomain Ω_1 and Ω_2, assorted with Dirichlet boundary conditions on $\delta\Omega$, defined as the boundary of Ω, and where $[\![\cdot]\!]$ means $\cdot_1 - \cdot_2$. The domain Ω can have an arbitrary shape. In the whole paper, we assume that the solution u of problem (1)-(3) exists and is smooth enough so that our truncation error analyses are valid. We assume, by convention, that the coefficient k is larger in Ω_2 than in Ω_1 ($k_2 > k_1$), and that the vector $\mathbf{n}$ is the outside normal for the subdomain Ω_2. These conventions will be used in the convergence proof. Note that others configurations than the one illustrated on this figure are possible, for instance, Ω_1 separated in several subdomains, and are all covered by our analysis.

This elliptic problem with discontinuities across an interface appears in numerous physical or biological models. Among the well-known applications are heat transfer, electrostatics, incompressible flows with discontinuous densities and viscosities [18], but similar elliptic problems arise for instance in tumour growth modelling, where one has to solve a pressure equation [3], or in the modelling of electric potential in biological cells: see for instance [4] or [12] and [13] where the mentioned numerical method was applied.

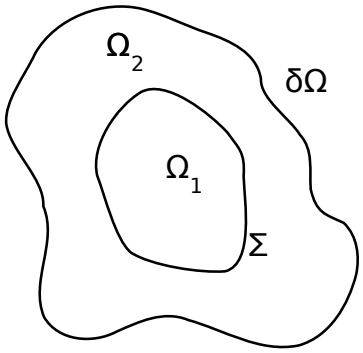

Figure 1: Geometry considered: two subdomains Ω_1 and Ω_2 separated by a complex interface Σ.

The method that we study is based on a finite-difference discretization and a dimension by dimension approach. In order to solve accurately the problem defined by equations (1) - (3) near the interface, additional unknowns are defined at the intersections of the interface with the grid, see Figure 2. These interface unknowns are used in the discretization of the elliptic operator near the interface, and avoid us to derive specific finite differences formulas containing jump terms, corrective terms, or needing the inversion of a linear system, as in many other second-order Cartesian methods. In order to solve the interface unknowns, the flux jump conditions are discretized and added to the linear system to solve. Jump

conditions and the coupling of the solution in the different subdomains are thus handled independently of the discretization of the elliptic equation.

In the following we will prove the convergence of the method in two cases: the original second-order method in one dimension, and a first-order version in two dimensions. This first-order version is based on the same ideas as the original method, but the discretization of the normal derivatives across the interface has only a first-order truncation error, instead of a second-order for the original method.

The proof of convergence is based on the monotonicity of the discretization matrix and a discrete maximum principle. Note that this monotonicity is not trivial for the second-order discretization, since the discretization matrix is not diagonally dominant, due to the discretization of the flux jump conditions across the interface. Then we obtain accurate estimates of the coefficients of the inverse matrix, block by block, in order to account for the different types of truncation errors, thanks to a technique presented in [6]. Combined to the truncation error expressed block by block, these estimates provide first- or second-order bounds on the numerical error.

2 Description of the numerical schemes

2.1 Interface representation and classification of grid points

In order to describe accurately the geometric configuration in the vicinity of the interface we use the level set method introduced by Osher and Sethian [21]. We refer the interested reader to [22], [23] and [20] for recent reviews of this method. The zero isoline of the level set function, defined by the signed function φ:

$$\varphi(x) = \begin{cases} dist_\Sigma(x) & \text{outside of the interface} \\ -dist_\Sigma(x) & \text{inside of the interface} \end{cases} \tag{4}$$

represents implicitely the interface Σ immersed in the computational domain.

The level-set, being a distance function, is defined and Lipshitz-continuous everywhere in the computational domain. However there can exist a subset of points of Ω of dimension 1 where φ is not differentiable. Everywhere else, it is twice differentiable. Moreover, we assume that the interface is smooth enough, so that there exists a positive real r_0 such that the level-set is twice differentiable for all x, y such that $|\varphi(x,y)| \leq r_0$.

A useful property of the level set function, where it is differentiable, is

$$\mathbf{n}(x) = \frac{\nabla\varphi(x)}{|\nabla\varphi(x)|}, \tag{5}$$

where $\mathbf{n}(x)$ is the outward normal vector of the isoline of φ passing on x. In this paper, the level-set is defined so that $\mathbf{n}$ is the outside normal for the subdomain Ω_2.

Considering the nodes used for discretizing the problem (1)-(3):

- The problem (1) - (3) is discretized on a uniform Cartesian grid covering $\Omega_1 \cup \Omega_2$, see Figure 3. The grid spacing is denoted h. The points on the cartesian grid are named either with letters such as P or Q, or with indices such as $M_{i,j} = (x_i, y_j) = (ih, jh)$ if one needs to have informations about the location of the point. We denote by u_{ij}^h the approximation of u at the point (x_i, y_j).

- We say that a grid point is irregular if it is neighboring the interface, that is, if the sign of φ changes between this point and at least one of its neighbors, see Figure 2. On the contrary, grid points that are not irregular are said regular grid points. The set of grid points located inside the domain Ω is denoted Ω_h. The set of regular grid nodes is denoted Ω_h^{**}, and the set of irregular grid nodes is denoted Ω_h^*.

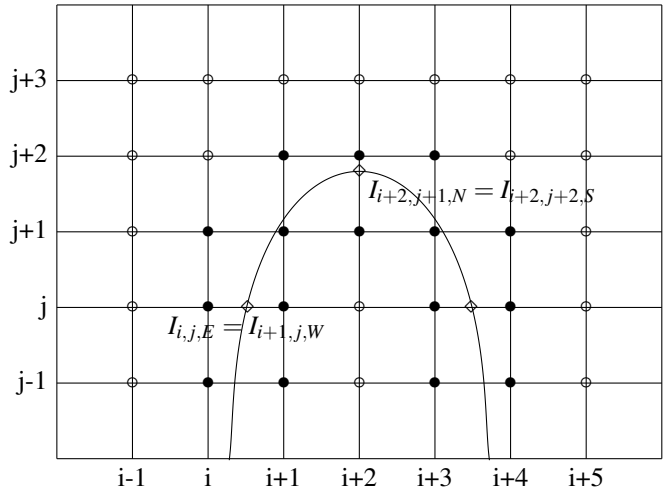

Figure 2: Example of geometrical configuration, with regular grid points (belonging to Ω_h^{**}) in white, irregular points (belonging to Ω_h^*) in black, and interface points (belonging to Σ_h) with the two possible notations.

- We define the following subsets, among regular grid points:
  - Ω_h^s: set of grid points that are regular and where the level-set is twice differentiable,
  - Ω_h^φ set of grid points that are regular and where the finite-difference formulas described in the following can not be applied because there is a lack of smoothness of φ and the stencil used for the discretization crosses this non-smooth region. Note that $\Omega_h^s \cup \Omega_h^\varphi = \Omega_h^*$
  - Ω_h^{**} the set of irregular grid points.
- The set of points located at the intersection of the axes of the grid and the interface Σ, which are called the interface points, is denoted Σ_h, see Figure 3 for an illustration. We also denote $\delta\Omega_h$ the set of points defined as the intersection between the grid and $\delta\Omega$. They are used to impose boundary conditions.

  We define the interface point $I_{i,j,\mathrm{E}} = (x_{i,j,\mathrm{E}}, y_j) = (x_{i,j,\mathrm{E}}, y_{i,j,\mathrm{E}})$ as the intersection of the interface and the segment $[M_{ij}M_{i+1j}]$, if it exists. Similarly, the interface points $I_{i,j,\mathrm{W}} = (x_{i,j,\mathrm{W}}, y_{i,j,\mathrm{W}})$, $I_{i,j,\mathrm{N}} = (x_{i,j,\mathrm{N}}, \tilde{y}_{i,j,\mathrm{N}})$ and $I_{i,j,\mathrm{S}} = (x_{i,j,\mathrm{S}}, \tilde{y}_{i,j,\mathrm{S}})$ are respectively defined as the intersections of the interface and the segments $[M_{i-1j}M_{ij}]$, $[M_{ij}M_{ij+1}]$ and $[M_{ij-1}M_{ij}]$. Let us remark that, with this notation, the same interface point is described in two different ways: for instance

$$I_{i,j,\mathrm{S}} = I_{i,j-1,\mathrm{N}} \text{ and } I_{i,j,\mathrm{E}} = I_{i+1,j,\mathrm{W}}.$$

  At each interface point we create two additional unknowns, called interface unknowns, and denoted by $u_{i,j,\gamma}^{1,h}$ and $u_{i,j,\gamma}^{2,h}$ with $\gamma = \mathrm{E}, \mathrm{W}, \mathrm{N}$ or S. The interface unknowns carry the values of the numerical solution on each side of the interface.

2.2 Second-order discretization in one dimension

The one-dimensional version of the second-order numerical scheme will be studied in detail in the paper. Therefore, to clarify the notations, we briefly present it in this subsection.

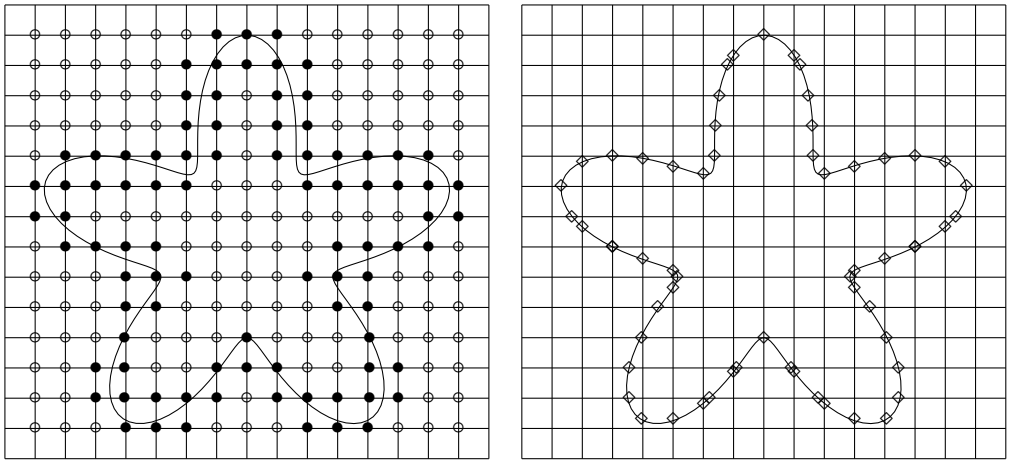

Figure 3: Left: regular nodes (belonging to Ω_h^{**}) described by circles $\circ$, irregular nodes (belonging to Ω_h^{*}) described by bullets $\bullet$, right: nodes belonging to Σ_h.

- Discrete elliptic operator on a grid point M_i

  We use the standart three point stencil: M_i and its nearest neighbors in each direction, either grid points or interface points. We denote u_E the value of the solution on the nearest point in the east direction, and x_E its coordinate. Similarly, we define u_W and x_w in the west direction. The discretization at point M_i reads

$$-\Big(\nabla.(k\nabla u)\Big)_i^h \quad = \quad -k\frac{2}{x_E-x_W}\Big(\frac{u_E-u_i}{x_E-x_i}-\frac{u_i-u_W}{x_i-x_W}\Big). \tag{6}$$

  The truncation error of this discretization is second-order accurate if all the points involved are grid points, and first-order otherwise.

- Discrete jump conditions across the interface

  On Figure 4, we present a prototypical situation around the interface: the interface point $x_{int} = x_{k,E}$ is located between the grid points x_k and x_{k+1} and we denote $dh = x_{k+1} - x_{int}$. We assume for instance that the subdomain Ω_2 is located on the left side of the interface, and Ω_1 on the right side. The normal to the interface is oriented from the left to the right.

  The left and right normal derivatives at the interface are computed with second-order formulas using three non-equidistant points:

$$\begin{aligned}(\partial_n u^1)_{int}^h &= \frac{1+2d}{d(d+1)h}(u_{k+1}^h - u_{k,E}^{1,h}) - \frac{d}{(1+d)h}(u_{k+2}^h - u_{k+1}^h),\\ (\partial_n u^2)_{int}^h &= \frac{3-2d}{(1-d)(2-d)h}(u_{k,E}^{2,h} - u_k^h) - \frac{1-d}{(2-d)h}(u_k^h - u_{k-1}^h).\end{aligned}$$

  We express the jump conditions at point x_{int} as

$$k_2(\partial_n u^2)_{int}^h - k_1(\partial_n u^1)_{int}^h = \beta(x_{int}), \tag{7}$$

$$u_{k,E}^{2,h} - u_{k,E}^{1,h} = \alpha(x_{int}). \tag{8}$$

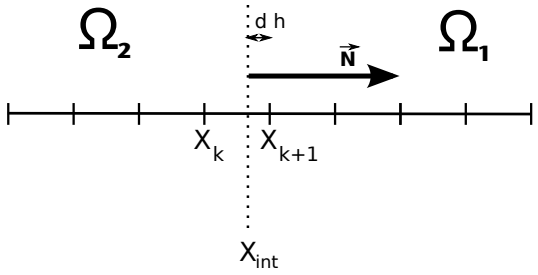

Figure 4: Geometrical configuration near the interface in one dimension.

2.3 First-order discretization in two dimensions

The numerical solution is obtained by solving the linear system arising from the following equations:

- Discrete elliptic operator

  We use a standard five point stencil. We use the grid point $M_{i,j}$ and its nearest neighbors in each direction: interface or grid points. More precisely, we denote u_S^h the value of the solution on the nearest point in the south direction, with coordinates (x_S, y_S). Similarly, we define u_N^h, u_W^h and u_E^h and the associated coordinates (x_N, y_N), (x_W, y_W) and (x_E, y_E). The discretization reads

$$-\Big(\nabla.(k\nabla u)\Big)^h(x_i,y_j) = -\Big(\nabla.(k\nabla u)\Big)^h_{i,j} = -k\frac{\dfrac{u_N^h-u_{ij}^h}{x_N-x_i}-\dfrac{u_{ij}^h-u_S^h}{x_i-x_S}}{\dfrac{x_N-x_S}{2}} - k\frac{\dfrac{u_E^h-u_{ij}^h}{y_E-y_j}-\dfrac{u_{ij}^h-u_W^h}{y_j-y_W}}{\dfrac{y_E-y_W}{2}}. \quad (9)$$

  The truncation error of this discretization is second-order accurate if all the points involved are grid points, that is, on regular grid points, and first-order on irregular grid points.

- Discrete jump conditions across the interface

  We discretize the jump conditions (2) and (3) at each interface point $I_{i,j,\gamma}$, with $\gamma = N,S,W,E$.

$$u_{i,j,\gamma}^{2,h} - u_{i,j,\gamma}^{1,h} = \alpha(I_{i,j,\gamma}), \quad (10)$$

$$k_2(\partial_n u^2)_{i,j,\gamma}^h - k_1(\partial_n u^1)_{i,j,\gamma}^h = \beta(I_{i,j,\gamma}). \quad (11)$$

  The discretization of the normal derivatives depends of the local geometry of the interface. On Figure 5 one can observe the four cases that are met in practice, if h is small enough, on each side of the interface. The first intersection between the normal to the interface and the grid is located on a segment: either $[M_{i,j}, M_{i,j-1}]$, or $[M_{i,j-1}, M_{i+1,j-1}]$, or $[M_{i,j}, M_{i,j+1}]$, or $[M_{i,j+1}, M_{i+1,j+1}]$.

  The discrete normal derivative is computed as the normal derivative of the linear interpolant of the numerical solution on the triangle composed of the interface point $I_{i,j,\gamma}$ and the aforementioned segment. If we denote K this triangle, $a_1 = (x_1, y_1)$, $a_2 = (x_2, y_2)$ and $a_3 = (x_3, y_3)$ its vertices, and u_1, u_2 and u_3 the values on these vertices, the basis functions on the vertices for the linear interpolation write

$$\lambda_j(x,y) = \alpha_j x + \beta_j y + \gamma_j, \ j = 1,2,3,$$

with

$$\alpha_j = \frac{y_k - y_i}{(x_j - x_k)(y_j - y_i) - (x_j - x_i)(y_i - y_k)},$$
$$\beta_j = \frac{x_i - x_k}{(x_j - x_k)(y_j - y_i) - (x_j - x_i)(y_i - y_k)},$$
$$\gamma_j = \frac{x_k y_i - x_i y_k}{(x_j - x_k)(y_j - y_i) - (x_j - x_i)(y_i - y_k)},$$

(n_x, n_y) being an approximation of the vector normal to the interface at point $I_{i,j,\gamma}$. With these notations, the approximation of the normal derivative writes

$$(\partial_n u)^h_{i,j,\gamma} = (u_1\,\alpha_1 + u_2\,\alpha_2 + u_3\,\alpha_3)n_x + (u_1\,\beta_1 + u_2\,\beta_2 + u_3\,\beta_3)n_y.$$

This discretization is only first-order accurate because it is based on a linear interpolation.

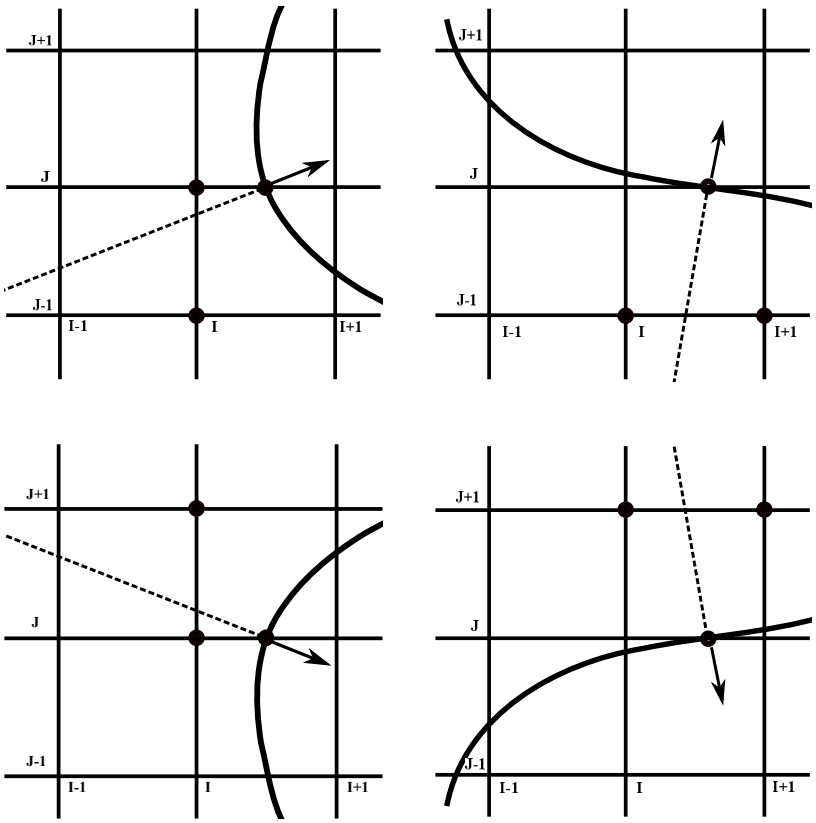

Figure 5: All possible stencils for the first-order flux discretization on the left side of the interface, with points involved in the discretization signaled by black circles.

2.4 Discretization matrix

In the following we denote A_h the matrix of the linear system described in the previous subsections, in one or two dimensions. We replace the variables $u^{2,h}_{i,j,\gamma}$ by $u^{1,h}_{i,j,\gamma} + \alpha(I_{i,j,\gamma})$ in the equations (7) or (11), and

(6) or (9), in order to eliminate the jump conditions (10) or (8) from the linear system. Because the jump conditions (10) or (8) are expressed exactly, this does not change the truncation errors for these equations.

We rewrite the whole linear system by separating the array of interface unknowns ($\mathbf{u_{int}}$) from the array of grid unknowns ($\mathbf{u_g}$), and among these unknowns, the unknowns in the subdomain Ω_1 ($\mathbf{u_g^1}$) from the unknowns in the subdomain Ω_2 ($\mathbf{u_g^2}$). This leads to

$$A_h\mathbf{u} = \left(\begin{array}{cc|c} -\Delta_1 & 0 & -\Delta_{int}^1 \\ 0 & -\Delta_2 & -\Delta_{int}^2 \\ \hline F_1 & F_2 & F_{int} \end{array}\right) \left(\begin{array}{c} \mathbf{u_g^1} \\ \mathbf{u_g^2} \\ \hline \mathbf{u_{int}} \end{array}\right) = \left(\begin{array}{c} f_1 + g_1(\alpha) \\ f_2 + g_2(\alpha) \\ \beta + g_3(\alpha) \end{array}\right) = F,$$

with

- Δ_1 and Δ_{int}^1 (resp. Δ_2 and Δ_{int}^2) the blocks corresponding to the discretization of the elliptic operator on subdomain Ω_1 (Ω_2),
- the arrays F_1, F_2 and F_{int} accounting for the contributions from grid points and interface points to the discretization of flux jump conditions (7) or (11).
- the terms f_1 and f_2 containing the source terms and the terms corresponding to Dirichlet boundary conditions,
- the terms $g_i(\alpha)$, $i = 1,2,3$, accounting for the presence in the right-hand side of a term depending on $\alpha(I_{i,j,\gamma})$ because of the elimination of the variable $u_{i,j,\gamma}^2$.

The local error array $\mathbf{e}$ and the consistency error array τ obey the same linear relationship as the numerical solution and the source terms:

$$A_h\mathbf{e} = \tau,$$

or equivalently

$$\left(\begin{array}{cc|c} -\Delta_1 & 0 & -\Delta_{int}^1 \\ 0 & -\Delta_2 & -\Delta_{int}^2 \\ \hline F_1 & F_2 & F_{int} \end{array}\right) \left(\begin{array}{c} e_g^1 \\ e_g^2 \\ \hline e_{int}^1 \end{array}\right) = \left(\begin{array}{c} \tau_g^1 \\ \tau_g^2 \\ \tau_{int}^1 \end{array}\right).$$

3 Convergence proof in two dimensions for the first-order version of the method

The sketch of the convergence proof is the following: first we prove the monotonicity of the discretization matrix, then we use it to apply a discrete maximum principle to the matrix, and obtain estimates on the coefficients of the inverse matrix, block by block.

3.1 Monotonicity of the discretization matrix

Here we aim to prove that A_h is monotone, that is, that all the coefficients of the inverse matrix of A_h are non-negative. Let $\mathbf{v}$ be an array of size $N + N_{int}$, corresponding to N grid points and N_{int} interface unknowns, such that all coefficients of $A_h\mathbf{v}$ are non-negative, which we denote $A_h\mathbf{v} \geq 0$. We aim to prove that all coefficients of $\mathbf{v}$ are non-negative.

To this purpose, we will use the following remark: *with the notations of Figure 6, if the minimum of* $\mathbf{v}$ *is located on an interface point, then at this interface point the discretized left normal derivative (in* Ω_1*) is negative and the discretized right normal derivative (in* Ω_2*) is positive.*

Indeed, the approximation of the normal derivative is constant, because it computed from a linear interpolation on a triangle. If the minimum of **v** is located on the considered interface point, then the left normal derivative at this interface point is negative and the right normal derivative at this interface point is positive. Moreover, if the approximated normal derivative is zero, then the three points values involved in the stencil are equal.

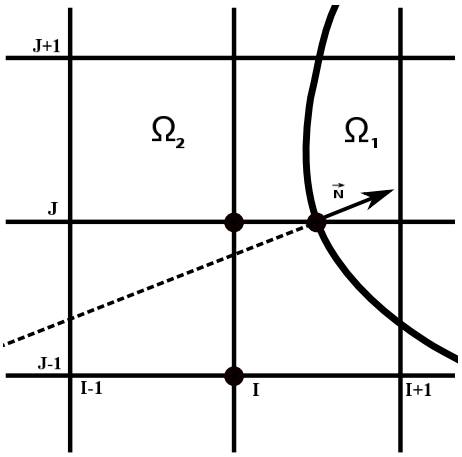

Figure 6: Geometrical configuration near the interface in two dimensions.

Now we consider the minimum of **v** in the whole domain, interface points included. This value can either be located on a grid point in one of the subdomains Ω_1 or Ω_2, or on an interface point.

- If the minimum is located on one border of the computational domain

  We assume for instance that the minimum of **v** is $v_{1,j}$, located on the grid point $M_{1,j}$, such that $M_{2,j}$, $M_{1,j+1}$ and $M_{1,j-1}$ also belong to the computational domain. Therefore, the boundary is located on the left side of $M_{1,j}$. The other cases would be treated the same way. The elliptic operator inequality on this grid point yields:

  $$\frac{4v_{1,j} - v_{2,j} - v_{1,j+1} - v_{1,j-1}}{h^2} \geq 0,$$

  then we have $4v_{1,j} \geq v_{2,j} + v_{1,j+1} + v_{1,j-1} \geq 3v_{1,j}$ and thus $v_{1,j} \geq 0$. Therefore all values of **v** are non-negative.

- If the minimum is reached on a grid point in one subdomain sharing at least one point with $\delta\Omega$

  In this case we denote (i_0, j_0) the indices of the smallest component of **v**. We assume the grid point is a regular grid point (otherwise the formula would have slightly different weights, but the reasoning would be the same). Using the elliptic operator inequality on this point we can write:

  $$4v_{i_0,j_0} - v_{i_0+1,j_0} - v_{i_0-1,j_0} - v_{i_0,j_0+1} - v_{i_0,j_0-1} \geq 0,$$

  we deduce that $v_{i_0+1,j_0} = v_{i_0-1,j_0} = v_{i_0,j_0+1} = v_{i_0,j_0-1} = v_{i_0,j_0}$. Using similar inequalities of the elliptic operator in all the subdomain, we deduce that all values in the subdomain, including the boundary values, are equal to v_{i_0,j_0}. We use now the reasoning of the last paragraph to conclude that all values of **v** are non-negative.

- If the minimum is reached on a grid point in one subdomain which does not share any point with $\delta\Omega$

  We use the notations and geometrical configuration of Figure 4. We assume, without loss of generality, that the subdomain is Ω_1 and we denote (i_0, j_0) the indices of the smallest component of $\mathbf{v}$. We assume the grid point is a regular grid point (otherwise the formula would have slightly different weights, but the reasoning would be the same). Writing the elliptic operator inequality on this point, we obtain

  $$4v_{i_0,j_0} - v_{i_0+1,j_0} - v_{i_0-1,j_0} - v_{i_0,j_0+1} - v_{i_0,j_0-1} \geq 0,$$

  and we deduce that $v_{i_0+1,j_0} = v_{i_0-1,j_0} = v_{i_0,j_0+1} = v_{i_0,j_0-1} = v_{i_0,j_0}$. Using similar inequalities of the elliptic operator in all the subdomain, we deduce that all values in the subdomain, including the interface values, are equal to the minimum value v_{i_0,j_0}.

  Let us consider one of these interface values. As noticed previously, the fact that all values are equal in the subdomain implies that the normal derivative at the interface point is zero. Due to the fact that $A_h v \geq 0$, we can write on this interface point:

  $$0 = k^1(\partial_n v^1)^h_{i,j,\gamma} \quad \leq \quad k^2(\partial_n v^2)^h_{i,j,\gamma}.$$

  On the other side, because the minimum value is reached on this interface point, we have also

  $$(\partial_n v^2)^h_{i,j,\gamma} \geq 0.$$

  Consequently, $(\partial_n v^1)^h_{i,j,\gamma} = (\partial_n v^2)^h_{i,j,\gamma} = 0$, and the values of the grid points involved in the stencil for $(\partial_n v^2)^h_{i,j,\gamma}$ are equal to the value of the interface point. It means that there are two grid points in the subdomain Ω_2 where the minimum value is reached.

  In this paper we have considered so far that there are only two subdomains. Therefore, we know that the subdomain Ω_2 has a non-void intersection with $\delta\Omega$, and we can apply the reasoning of the last paragraph to conclude. In the case where more subdomains were considered, we would distinguish whether the subdomain Ω_2 has a non-void intersection with $\delta\Omega$ or not. If not the case, then we would apply again the reasoning of this paragraph, switching from subdomains to subdomains, until finding a subdomain whose intersection with $\delta\Omega$ is non empty.

- If the minimum is located on one interface point

  On this interface point, following the notations of Figure 4 we have the two relationships

  $$\begin{aligned}(\partial_n v^2)^h_{i,j,\gamma} &\leq 0,\\ (\partial_n v^1)^h_{i,j,\gamma} &\geq 0.\end{aligned}$$

  Furthermore, we know that

  $$k^2(\partial_n v^2)^h_{i,j,\gamma} - k^1(\partial_n v^1)^h_{i,j,\gamma} \quad \geq \quad 0.$$

  We infer from the previous inequalities that $(\partial_n v^2)^h_{i,j,\gamma} = (\partial_n v^1)^h_{i,j,\gamma} = 0$. Therefore there are at least two grid points in each subdomain where the minimum value is reached. We can then follow the reasoning of one of the two last paragraphs.

We have proven that if $A_h v$ is non-negative, then v is also non-negative. This property has two implications:

- A_h is invertible. Indeed, let us assume that an array v is such that $A_h v = 0$. It means that both $A_h v$ and $A_h(-v)$ are non-negative. Consequently, we have $v \geq 0$ and $-v \geq 0$, thus $v = 0$.
- All values of A_h^{-1} are non-negative. Indeed, the property is equivalent to say that, for any y non-negative, we have also $A_h^{-1} y$ non-negative, which exactly means that all values of A_h^{-1} are non-negative.

3.2 Notations and reminder of the method of Ciarlet

In the following, the letters P and Q represent either discretization points (on the grid or on the interface) or their indices in the global numerotation of the matrix. For instance, we denote $u(P)$ the coefficient of the row of u with the same index than the point P. Similarly, $A_hU(P)$ represents the coefficient of the P-th row of the array A_hU, and $A_h(P,Q)$ is the coefficient of the P-th row and Q-th column of the matrix A_h. We also define respectively by $A_h(:,Q)$ and $A_h(P,:)$ the Q-th column and the P-th row of the matrix A_h.

For each $Q \in \Omega_h$, define the discrete Green's function $G_h(:,Q) = \Big(G_h(P,Q)\Big)_{P\in\Omega_h\cup\Sigma_h}$ as the solution of the discrete problem:

$$\left\{ \begin{array}{l} A_hG_h(:,Q)(P) = \left\{ \begin{array}{ll} 0, & P \neq Q \\ 1, & P = Q \end{array} \right. \quad P \in \Omega_h, \\ \qquad G_h(P,Q) = 0, \quad P \in \delta\Omega_h \cup \Sigma_h. \end{array} \right. \tag{12}$$

The matrix A_h being monotone, all values of $G_h(P,Q)$ are positive. With this definition of G_h we can write the solution of the numerical problem as a sum of the source terms multiplied by the values of the discrete Green function:

$$u_h(P) = \sum_{Q\in\Omega_h\cup\Sigma_h} G_h(P,Q)\,(A_hu_h)(Q), \quad \forall P \in \Omega_h \cup \Sigma_h.$$

Now we present the result of [6], based on a discrete maximum principle, slightly modified to be adapted to our discretization matrix. Let S be a subset of points, W a discrete function with $W \equiv 0$ on $\delta\Omega_h$, and $\alpha > 0$ such that:

$$\left\{ \begin{array}{l} (A_hW)(P) \geq 0 \quad \forall P \in \Omega_h \cup \Sigma_h, \\ (A_hW)(P) \geq \alpha^{-i} \quad \forall P \in S. \end{array} \right.$$

Then

$$\sum_{Q\in S} G_h(P,Q) \leq \alpha^i W(P), \quad \forall P \in \Omega_h \cup \Sigma_h.$$

Proof. Using the definition of the discrete Green function, we can write

$$\Big(A_h \sum_{Q\in S} G_h(:,Q)\Big)(P) = \left\{ \begin{array}{ll} 1 & \text{if } P \notin S, \\ 0 & \text{if } P \in S. \end{array} \right.$$

Therefore,

$$A_h\Big(W - \alpha^{-i} \sum_{Q\in S} G_h(:,Q)\Big)(P) \geq 0, \quad \forall P \in \Omega_h \cup \Sigma_h.$$

As all coefficients of the inverse of A_h are non-negative, it leads to

$$W(P) - \alpha^{-i} \sum_{Q\in S} G_h(P,Q) \geq 0, \quad \forall P \in \Omega_h \cup \Sigma_h,$$

and finally we obtain an estimate of $\sum_{Q\in S} G_h(:,Q)$ in terms of the coefficients of W:

$$\sum_{Q\in S} G_h(P,Q) \leq \alpha^i W(P), \quad \forall P \in \Omega_h \cup \Sigma_h.$$

■

3.3 Convergence proof

Here we prove the first-order convergence of the variant of the method presented in subsection 2.3, in two dimensions. We first obtain linear relationships between the sums of the coefficients of the blocks of the inverse matrix corresponding to Ω_h^{**}, Ω_h^r, Ω_h^φ and Σ_h. Then we combine these relationships in order to obtain the desired estimates. In this subsection, strictly positive constants independent of h are denoted by C_i, with $i = 1, 2, ...$

3.3.1 Coupled estimates for grid points and interface points

We define the function f as:

$$f(x,y) = B - e^{-A\varphi(x,y)},$$

with φ the level-set function defined as the signed distance to the interface, negative in Ω_2 and positive in Ω_1.

The function f satisfies at each point where it is twice differentiable:

$$-\Big(\nabla.(k\nabla f)\Big)(x,y) = k\Big[A^2\Big(\underbrace{(\partial_x\varphi)^2 + (\partial_y\varphi)^2}_{=1}\Big) - A\nabla.(\nabla\varphi)(x,y)\Big]e^{-A\varphi(x,y)},$$

because φ is the signed distance function. Moreover, because of (5),

$$\partial_n f(x,y) = Ae^{-A\varphi}\underbrace{(\partial_x\varphi\, n_x + \partial_y\varphi\, n_y)}_{=1}, \forall (x,y) \in \Sigma.$$

We choose A and B such that: $kA^2 - A\nabla.(k\nabla\varphi)(x,y) \geq 1, \forall (x,y) \in \Omega$, and $B - e^{-A||\varphi||_\infty} > 0$, with $||\varphi||_\infty = \max_\Omega |\varphi|$. With such values of A and B, we can write for (x,y) where φ is differentiable:

$$f(x,y) \geq 0, \tag{13}$$

$$-\Big(\nabla.(k\nabla f)\Big)(x,y) \geq ke^{-A||\varphi||_\infty} \geq 0, \tag{14}$$

$$k^2\partial_n f(x,y) - k^1\partial_n f(x,y) \geq (k^2 - k^1)Ae^{-A||\varphi||_\infty}, \quad \text{if } (x,y) \in \Sigma. \tag{15}$$

However, for points where the level-set is not differentiable these relationships are not valid and neither is their discrete version. To circumvent this problem, we will regularize the function f.

We denote by $B(x_M, y_M, \eta)$ the sphere of center $M = (x_M, y_M)$ and radius η. First, we remark that, because the interface Σ is smooth and f is smooth near Σ, there exists a positive real η such that for each point M belonging to Σ, and for all $(x,y) \in B(x_M, y_M, \eta)$,

$$\begin{aligned} k^2\partial_n f(x,y) - k^1\partial_n f(x,y) &\geq \frac{1}{2}\Big[k^2\partial_n f(x_M,y_M) - k^1\partial_n f(x_M,y_M)\Big], \\ &\geq \frac{1}{2}(k^2 - k^1)Ae^{-A||\varphi||_\infty}. \end{aligned} \tag{16}$$

We consider the following function, positive and infinitely differentiable with compact support:

$$g(x,y) = \begin{cases} \exp\left(-\frac{1}{1-r^2}\right) & \text{if } r^2 \leq 1, \quad \text{with } r^2 = \frac{x^2+y^2}{\eta^2}, \\ 0 & \text{elsewhere.} \end{cases}$$

We define the regularized version of f as

$$F(x,y) = \int_{\mathbb{R}^2} g(x-s, y-t) f(s,t)\, ds\, dt.$$

If we apply the discrete elliptic operator (9) to F we get for instance in the case of a regular point $M_{i,j}$:

$$\begin{aligned}-\Big(\nabla.(k\nabla F)\Big)^h_{i,j} &= \frac{k}{h^2}\Big(4F(x_i,y_j)-F(x_i+h,y_j)-F(x_i-h,y_j)-F(x_i,y_j+h)-F(x_i,y_j-h)\Big),\\ &= \int_{\mathbb{R}^2}\Big(-\nabla.(k\nabla g)\Big)^h(x_i-s,y_i-t)f(s,t)ds\,dt.\end{aligned}$$

A similar formula would be obtained in the case of an irregular grid point. The term $\Big(-\nabla.(k\nabla g)\Big)^h$ is consistent with $-\nabla.(k\nabla g)$ at first or second-order (depending if we consider a regular or irregular grid point), therefore there exists a positive constant C_1 depending only on f, g, k and Ω, such that

$$-\Big(\nabla.(k\nabla F)\Big)^h_{i,j} \geq -C_1, \quad \forall M_{i,j}\in\Omega_h.$$

This estimate is valid at every grid point in the domain, and notably for grid points in Ω_h^φ. However, better estimates can be obtained for grid points belonging to Ω_h^s, where φ is smooth. With a simple change of variables,

$$F(x+h,y)=\int_{\mathbb{R}^2} g(x+h-s,y-t)f(s,t)ds\,dt=\int_{\mathbb{R}^2} g(x-s,y-t)f(s+h,t)ds\,dt.$$

We apply the same treatment on every term appearing in the discretization of the elliptic operator and obtain:

$$-\Big(\nabla.(k\nabla F)\Big)^h_{i,j}=-\int_{\mathbb{R}^2} g(x_i-s,y_i-t)\Big(\nabla.(k\nabla f)\Big)^h(s,t)ds\,dt.$$

where $\Big(\nabla.(k\nabla f)\Big)^h(s,t)$ stands for a discretization similar to $\Big(\nabla.(k\nabla f)\Big)^h_{i,j}$, but shifted from $M_{i,j}$ to (s,t). We know that $\nabla.(k\nabla f)$ is positive for points where the level-set is differentiable. Therefore, there exists a strictly positive constant C_2, depending only on f, g, k and Ω, such that

$$-\Big(\nabla.(k\nabla F)\Big)^h_{i,j}\geq C_2, \forall M_{i,j}\in\Omega_h^s. \tag{17}$$

The same reasoning is valid for the discretization of the jump of fluxes at the interface:

$$\begin{aligned}k_2(\partial_n F^2)^h_{i,j,\gamma}-k_1(\partial_n F^1)^h_{i,j,\gamma} &= \int_{\mathbb{R}^2} g(x_{i,j,\gamma}-s,y_{i,j,\gamma}-t)\Big(k_2(\partial_n f^2)^h-k_1(\partial_n f^1)^h\Big)(s,t)ds\,dt,\\ &= \int_{B(x_{i,j,\gamma},y_{i,j,\gamma},\eta)} g(x_{i,j,\gamma}-s,y_{i,j,\gamma}-t)\Big(k_2(\partial_n f^2)^h-k_1(\partial_n f^1)^h\Big)(s,t)ds\,dt.\end{aligned}$$

Here again, the notation $\Big(k_2(\partial_n f^2)^h-k_1(\partial_n f^1)^h\Big)(s,t)$ denotes a discretization on a stencil similar to $k_2(\partial_n f^2)^h_{i,j,\gamma}-k_1(\partial_n f^1)^h_{i,j,\gamma}$, but shifted from $I_{i,j,\gamma}$ to (s,t). Therefore, because of the definition of g and η and (16), we can write

$$k_2(\partial_n f^2)^h_{i,j,\gamma}-k_1(\partial_n f^1)^h_{i,j,\gamma}\geq \underbrace{\frac{1}{2}(k_2-k_1)Ae^{-A||\varphi||_\infty}\int_{B(x_{i,j,\gamma},y_{i,j,\gamma},\eta)} g(x-s,y-t)ds\,dt}_{=C_3}>0.$$

To sum up the previous lines, if we denote W the array of the values of F discretized on the grid and interface points, with $W \equiv 0$ on $\delta\Omega_h$, there exists three strictly positive constants, C_1, C_2 and C_3, depending only on f, g, k and Ω, such that

$$\begin{aligned}
&(A_h W)(P) \geq -C_1, \quad \forall P \in \Omega_h^\varphi, \\
&(A_h W)(P) \geq C_2, \quad \forall P \in \Omega_h^{**} \cup \Omega_h^s, \\
&(A_h W)(P) \geq C_3, \quad \forall P \in \Sigma_h.
\end{aligned}$$

Using lemma (3.2), it means that:

$$C_2 \sum_{Q \in \Omega_h^{**} \cup \Omega_h^s} G_h(:,Q) + C_3 \sum_{Q \in \Sigma_h} G_h(:,Q) \leq W + C1 \sum_{Q \in \Omega_h^\varphi} G_h(:,Q). \tag{18}$$

3.3.2 Estimates for grid points in Ω_h^φ

Let $P = (x_n, y_m)$ be a grid point belonging to Ω_h^φ. We consider here the fonction

$$\tilde{F}_P(x,y) = \ln\left(\frac{C}{r_P(x,y,h)}\right),$$

with $r_P(x,y) = \sqrt{(x-x_n)^2 + (y-y_m)^2 + h^2}$, and C such that $\tilde{F}_P(x,y) > 0$ for all $(x,y) \in \Omega$.

Without loss of generality, we assume in the following that $x_n = y_m = 0$. We can prove that for every regular grid point $M_{i,j}$

$$-\Big(\nabla.(k\nabla\tilde{F}_P)\Big)_{i,j}^h \geq 0, \tag{19}$$

and in particular, when applied on the point P itself,

$$-\Big(\nabla.(k\nabla\tilde{F}_P)\Big)_{n,m}^h \geq \frac{C_4}{h^2}, \tag{20}$$

with C_4 a strictly positive constant. Indeed, the finite difference formula applied to $\tilde{F}_P$ on a regular grid point gives:

$$\begin{aligned}
-\Big(\nabla.(k\nabla\tilde{F}_P)\Big)_{i,j}^h &= \frac{k}{h^2} ln\Big(\frac{r_{i-1,j}\, r_{i+1,j}\, r_{i,j-1}\, r_{i,j+1}}{r_{i,j}^4}\Big), \\
&= \frac{k}{2h^2} ln\Big(\frac{\Big[(x+h)^2+y^2+h^2\Big]\Big[(x-h)^2+y^2+h^2\Big]\Big[x^2+(y+h)^2+h^2\Big]\Big[x^2+(y-h)^2+h^2\Big]}{(x^2+y^2+h^2)^4}\Big).
\end{aligned}$$

Moreover,

$$\begin{aligned}
\Big[(x+h)^2+y^2+h^2\Big]\Big[(x-h)^2+y^2+h^2\Big] &= (x^2+y^2+h^2)^2 + 3h^4 - 2h^2x^2 + 2h^2y^2, \\
\Big[x^2+(y+h)^2+h^2\Big]\Big[x^2+(y-h)^2+h^2\Big] &= (x^2+y^2+h^2)^2 + 3h^4 - 2h^2y^2 + 2h^2x^2.
\end{aligned}$$

Therefore

$$-\Big(\nabla.(k\nabla\tilde{F}_P)\Big)_{i,j}^h = \frac{k}{2h^2} ln\Big(\frac{[(x^2+y^2+h^2)^2+3h^4]^2 - 4h^4(x^2-y^2)^2}{(x^2+y^2+h^2)^4}\Big).$$

We develop the term and remark that

$$\Big[(x^2+y^2+h^2)^2+3h^4\Big]^2-4h^4(x^2-y^2)^2\geq(x^2+y^2+h^2)^4,$$

which gives us (19). The relationship (20) is directly obtained by using $x_i=y_j=0$ in the formula.

On irregular grid points, we simply notice that, with Taylor expansions, one can prove that there exists a positive constant C_5 such that

$$-\Big(\nabla.(k\nabla\tilde{F}_P)\Big)_{i,j}^h\geq -C_5,\quad \forall M_{i,j}\in\Omega_h^{**}.$$

On the other side, the discretization of the jump of fluxes with the function $\tilde{F}_P$ is not necessarily positive. However, as the interface points are at a distance bounded independently of h from the considered point P, the value of $\partial_n\tilde{F}_P$ is bounded independently of h. Consequently there exists a positive constant C_6 such that

$$k_2(\partial_n\tilde{F}_P^2)_{i,j,\gamma}^h-k_1(\partial_n\tilde{F}_P^1)_{i,j,\gamma}^h\geq -C_6,\quad \forall I_{i,j,\gamma}\in\Sigma_h. \tag{21}$$

To sum up the previous lines, if we denote $\tilde{W}_P$ the array of the values of $\tilde{F}_P$ discretized on the grid and interface points, with $\tilde{W}_P\equiv 0$ on $\delta\Omega_h$, there exists three strictly positive constants, C_4, C_5 and C_6, such that

$$\tilde{W}_P(:)\geq\frac{C_4}{h^2}G_h(:,P)-C_6\sum_{Q\in\Sigma_h}G_h(:,Q)-C_5\sum_{Q\in\Omega_h^{**}}G_h(:,Q),$$

or equivalently

$$C_4G_h(:,P)\leq h^2\tilde{W}_P(:)+h^2C_6\sum_{Q\in\Sigma_h}G_h(:,Q)+h^2C_5\sum_{Q\in\Omega_h^{**}}G_h(:,Q). \tag{22}$$

We want to sum this relationship on all points P belonging to Ω_h^{φ}. Thus we need an upper bound for $\displaystyle\sum_{P\in\Omega_h^{\varphi}}\tilde{W}_P(:)$.

Let us notice that for every point Q, there are $N_i=O(1)$ points P belonging to Ω_h^{φ} such that $ih\leq r_P(Q)\leq(i+1)h$, with i between 1 and $O(N)$. Consequently,

$$\sum_{P\in\Omega_h^{\varphi}}\tilde{W}_P(Q)=\sum_{P\in\Omega_h^{\varphi}}\ln\Big(\frac{C}{r_P(Q)}\Big)\leq\underbrace{\sum_{i=1}^{O(N)}O(1)\ln\Big(\frac{C}{ih}\Big)}_{=O(N)},\forall Q\in\Omega_h.$$

Therefore, if we sum the inequality (22) on all grid points in Ω_h^{φ} we obtain

$$\sum_{P\in\Omega_h^{\varphi}}G_h(:,P)\leq O(h)+O(h)\frac{C_6}{C_4}\sum_{Q\in\Sigma_h}G_h(:,Q)+O(h)\frac{C_5}{C_4}\sum_{Q\in\Omega_h^{**}}G_h(:,Q). \tag{23}$$

We combine (18) and (23) to obtain:

$$C_2\sum_{Q\in\Omega_h^{**}\cup\Omega_h^s}G_h(:,Q)+C_3\sum_{Q\in\Sigma_h}G_h(:,Q)\leq||W||_\infty+C_1\Big(O(h)+O(h)\frac{C_6}{C_4}\sum_{Q\in\Sigma_h}G_h(:,Q)+O(h)\frac{C_5}{C_4}\sum_{Q\in\Omega_h^{**}}G_h(:,Q)\Big).$$

Therefore, if h is small enough, we obtain

$$\sum_{Q\in\Omega_h^{**}\cup\Omega_h^s} G_h(:,Q) \leq C_7, \tag{24}$$

$$\sum_{Q\in\Sigma_h} G_h(:,Q) \leq C_8, \tag{25}$$

$$\sum_{Q\in\Omega_h^\varphi} G_h(:,Q) \leq O(h). \tag{26}$$

3.3.3 Estimates for irregular grid points

We need a more accurate estimate for $\sum_{Q\in\Omega_h^{**}} G_h(:,Q)$. We define the function $\bar{f}$ by :

$$\bar{f}(x,y) = \begin{cases} B - e^{-A(\varphi(x,y)+h/2)} & \text{if } \varphi(x,y) \leq -h/2, \\ B - e^{A(\varphi(x,y)-h/2)} & \text{if } \varphi(x,y) \geq h/2, \\ B \quad \text{if } |\varphi(x,y)| \leq h, \end{cases}$$

with φ the level-set function, defined previously as the signed distance to the interface, negative in Ω_2 and positive in Ω_1.

The discrete normal derivative computed with this function is positive for the formula with points in Ω_2, and negative for points in Ω_1:

$$k^2(\partial_n \bar{f}^2)^h_{i,j,\gamma} - k^1(\partial_n \bar{f}^1)^h_{i,j,\gamma} \geq 0, \quad \forall M_{i,j,\gamma} \in \Sigma_h.$$

For points in Ω_h^r, the discrete elliptic operator satisfies, as in the first subsection:

$$-\Big(\nabla.(k\nabla\bar{f})\Big)^h_{i,j} \geq 0, \quad \forall M_{i,j} \in \Omega_h^r.$$

For grid points in Ω_h^φ, because the level-set function φ is at least Lipschitz continuous, we can write

$$-\Big(\nabla.(k\nabla\bar{f})\Big)^h_{i,j} \geq -\frac{C_9}{h}, \quad \forall M_{i,j} \in \Omega_h^\varphi.$$

On the irregular grid points, we can write

$$-\Big(\nabla.(k\nabla\bar{f})\Big)^h_{i,j} \geq \frac{C_{10}}{h}, \quad \forall M_{i,j} \in \Omega_h^{**}. \tag{27}$$

More precisely, the inequality (27) is obtained directly if $|\varphi(x_i,y_j)| \leq h/2$. Otherwise we obtain $-\Big(\nabla.(k\nabla\bar{f})\Big)^h_{i,j} \geq \frac{C_{10}}{h^2}$, and (27) still holds as a lower bound. Therefore, if we denote $\bar{W}$ the array of the values of $\bar{f}$ discretized on the grid and interface points, with $\bar{W} \equiv 0$ on $\delta\Omega_h$,

$$-\frac{C_9}{h}\sum_{Q\in\Omega_h^\varphi} G_h(:,Q) + \frac{C_{10}}{h}\sum_{Q\in\Omega_h^{**}} G_h(:,Q) \leq \bar{W}(:)$$

$$C_{10}\sum_{Q\in\Omega_h^{**}} G_h(:,Q) \leq C_9\sum_{Q\in\Omega_h^\varphi} G_h(:,Q) + h\bar{W}(:) \leq O(h). \tag{28}$$

3.3.4 Convergence result

Finally, we obtain an estimate of the local error on every point P in $\Omega_h \cup \Sigma_h$, with $\bar{u}$ the exact solution:

$$\begin{aligned}
|\bar{u}(P) - u_h(P)| &= |\sum_{Q\in\Omega_h} G_h(P,Q)\tau(Q)|, \\
&\leq |\sum_{Q\in\Omega_h^{**}} G_h(P,Q)\tau(Q)| + |\sum_{Q\in\Omega_h^{r}} G_h(P,Q)\tau(Q)| + |\sum_{Q\in\Omega_h^{\varphi}} G_h(P,Q)\tau(Q)| + |\sum_{Q\in\Sigma_h} G_h(P,Q)\tau(Q)|, \\
&\leq O(h)|\sum_{Q\in\Omega_h^{**}} G_h(P,Q)| + O(h^2)|\sum_{Q\in\Omega_h^{r}} G_h(P,Q)| + O(h^2)|\sum_{Q\in\Omega_h^{\varphi}} G_h(P,Q)| + O(h)|\sum_{Q\in\Sigma_h} G_h(P,Q)|, \\
&\leq O(h)O(h) + O(h^2)O(1) + O(h^2)O(h) + O(h)O(1) = O(h).
\end{aligned}$$

which proves that the numerical solution converges with first-order accuracy to the exact solution in L^∞-norm.

4 Convergence proof for the one-dimensional case

4.1 Monotonicy of the discretization matrix

Here we aim to prove that A_h is monotone in spite of the fact that the matrix A_h is not diagonally-dominant in the second-order version, due to the discretization terms near the interface. Let $\mathbf{v}$ be an array of size $N + N_{int}$ corresponding to N grid points and N_{int} interface unknowns such that $A_h\mathbf{v} \geq 0$. We prove that, if the minimum of $\mathbf{v}$ is located on an interface point x_{int} then, with the notations and orientation of the normal defined on Figure 4 then the left normal derivative at this interface point is negative and the right normal derivative at this interface point is positive. Once we have proven this property, the proof of monotonicity of the matrix is exactly the same as in two dimensions, so we do not re-write it. We use the notations defined on Figure 4 and we denote $v_{int} = \tilde{v}_{k,E}$.

Let us assume that the minimum of $\mathbf{v}$ is located on an interface point. The left normal derivative at x_{int} is discretized by

$$(\partial_n v^2)^h_{int} = \frac{3-2d}{(1-d)(2-d)h}(v_{int} - v_k) - \frac{1-d}{(2-d)h}(v_k - v_{k-1}).$$

By hypothesis $A_h\mathbf{v} \geq 0$ hence

$$-\Big(\frac{v_{int} - u_k}{(1-d)h} - \frac{v_k - v_{k-1}}{h}\Big) \geq 0,$$

therefore

$$(\partial_n v^2)^h_{x_{int}} \leq \frac{2-d}{(1-d)(2-d)h}(v_{int} - v_k) \leq 0.$$

Moreover, if one can prove that the normal derivative is zero, with the last inequality we can deduce that $v_k = v_{int}$. Similarly, the right normal derivative at x_{int} is discretized by

$$(\partial_n v^1)^h_{int} = \frac{1+2d}{d(d+1)h}(u_{k+1} - v_{int}) - \frac{d}{(1+d)h}(v_{k+2} - v_{k+1}).$$

By hypothesis $A_h\mathbf{v} \geq 0$ hence

$$-\Big(\frac{v_{k+2} - v_{k+1}}{h} - \frac{v_{k+1} - v_{int}}{dh}\Big) \geq 0,$$

therefore

$$(\partial_n v^1)^h_{x_{int}} \quad \geq \quad \frac{1+d}{d(d+1)h}(v_{k+1} - v_{int}) \geq 0.$$

Again, if the normal derivative is zero, then $v_{k+1} = v_{int}$.

4.2 Second-order convergence

With exactly the same reasoning than in subsection 3.3 we can prove the estimates (24), (25), (26) and (28). We use them to obtain an estimate of the local error on every point P in $\Omega_h \cup \Sigma_h$:

$$\begin{aligned}
|\bar{u}(P) - u_h(P)| &= |\sum_{Q\in\Omega_h} G_h(P,Q)\tau(Q)|, \\
&\leq |\sum_{Q\in\Omega_h^{**}} G_h(P,Q)\tau(Q)| + |\sum_{Q\in\Omega_h^{r}} G_h(P,Q)\tau(Q)| + |\sum_{Q\in\Omega_h^{\varphi}} G_h(P,Q)\tau(Q)| + |\sum_{Q\in\Sigma_h} G_h(P,Q)\tau(Q)|, \\
&\leq O(h)|\sum_{Q\in\Omega_h^{**}} G_h(P,Q)| + O(h^2)|\sum_{Q\in\Omega_h^{r}} G_h(P,Q)| + O(h^2)|\sum_{Q\in\Omega_h^{\varphi}} G_h(P,Q)| + O(h^2)|\sum_{Q\in\Sigma_h} G_h(P,Q)|, \\
&\leq O(h)O(h) + O(h^2)O(1) + O(h^2)O(h) + O(h^2)O(1) = O(h^2).
\end{aligned}$$

which proves that the numerical solution converges with second-order accuracy to the exact solution in L^∞-norm.

5 Discussion

Numerous numerical methods have been developed for solving the problem (1) - (3), leading to various orders of accuracy for the convergence:

- the pioneering work of Mayo in 1984 [19], where an integral equation was derived to solve elliptic interface problems with piecewise coefficients to second order accuracy in maximum norm,
- the very well known Immersed Interface Method (IIM) LeVeque and Li (1994) [14] (second order accurate in maximum norm), and its developments, among them: the fast IIM algorithm of Li [15] for elliptic problems with piecewise constant coefficients, the Explicit Jump Immersed Interface Method (EJIIM) by Wiegmann and Bube [24], the Decomposed Immersed Interface Method (DIIM) by Bethelsen [2], and the MIIM (maximum principle preserving) by Li and Ito [16].
- the Matched Interface and Boundary (MIB) method [27], [26], [25], introduced by Zhou *et al.* : the solution on each side of the interface is extended on fictitious points on the other side. These fictitious values are computed by iteratively enforcing the lowest order interface jump conditions. This method can provide finite-difference schemes of arbitrary high order.
- the Coupling Interface Method, proposed by Chern and Shu [5], where the discretizations on each subdomain are coupled through a dimension by dimension approach using the jump conditions.

All the methods cited above are second order accurate. Other classes of Cartesian methods also exist, only first order accurate for interface problems in the case of interface problems, but simpler to implement: Gibou *et al.* ([8], [9]). Recently, Guittet *et al.* proposed in [10] to add degrees of freedom close to the interface and use a Voronoi partition centered at each of these points to discretize the equations in a finite volume approach. Doing so, they obtain a symmetric positive definite linear system, and a second-order convergence of the solution.

Concerning the discretization requirements needed to get a second-order spatial convergence, it has been noted since the introduction of Cartesian grid methods that a $O(h)$ truncation error at the points near the interface is enough to get a $O(h^2)$ convergence in maximum norm if the discretization is second-order on the regular grid points. However, in the literature, only few works have been devoted to the study of the second-order convergence of Cartesian grid methods for interface problems. For one-dimensional methods, Huang and Li performed in [11] a convergence analysis of the IIM, using non-negative comparison functions, and in [24] Wiegmann and Bube presented a proof of convergence for one-dimensional problems with piecewise constant coefficients, using a detailed analysis and identification of the coefficients of the matrices involved. In [12], a convergence proof was established in one-dimension for a variant of the method studied in this paper, applied in the context of electropermeabilization models. But this proof was based on a row by row analysis of the discretisation matrix, in order to obtain estimates of the coefficients of the inverse matrix. This technique would not be tractable in two dimensions, due to its complexity. For two-dimensional methods, Beale and Layton [1] proved in two-dimensions the second-order convergence for piecewise constant diffusion coefficients, using the fact that a grid function located near the interface can be written as the divergence of a function smaller in norm, and Li and Ito proved in [16] the second-order convergence of their MIIM, using the maximum principle, but with a technical condition related to the location of the interface with respect to the grid point that is not always satisfied. In this paper, the proof is also based on a discrete maximum principle, but its exact contents differs significantly from the proof in [16] because the discretization is not the same, notably due to the presence of interface unknowns, which makes the monotonicity of the matrix a crucial step in the proof, and lead to a different application of the discrete maximum principle.

This result can be considered as a step toward the convergence proof of the second-order method. In future works, we aim to adapt the ideas presented here to prove stability and second-order convergence for the initial method [7].

6 Numerical validation

In this section we only provide numerical results for the first-order method in two dimensions. Indeed, the second-order method has already been validated in two-dimensions in [7], and consequently there is no need to show it in one dimension here. The following numerical results are not meant to assess good performances of the method or compare it to others methods of the literature, but simply to corroborate the analysis that we have performed.

In all the following test cases, we consider a square domain Ω consisting in the union of two subdomains Ω_1 and Ω_2 separated by an interface Σ. If not specified otherwise, $\Omega = [-1,1] \times [-1,1]$. We impose exact Dirichlet boundary conditions on the outer boundary of Ω.

6.1 Problem 1

It is a test case appearing in [27] (MIB method, case 3 of the tests on irregular interfaces) and [5] (CIM, example 4). We consider an elliptical interface Σ defined as:

$$(\frac{x}{18/27})^2 + (\frac{y}{10/27})^2 = 1.$$

The exact solution is:

$$u(x,y) = \begin{cases} e^x cos(y), \text{ inside } \Sigma, \\ 5e^{-x^2-\frac{y^2}{2}} \text{ otherwise.} \end{cases}$$

As in [27] we fix the diffusion coefficient $k = 1$ outside the interface, and $k = 10$ inside the interface. We observe a first-order convergence, as presented in Table 1.

N	L^∞ error	order
20	1.2497×10^{-1}	-
40	$5.83079213 \times 10^{-2}$	1.10
80	3.0542764×10^{-2}	1.02
160	1.3751638×10^{-2}	1.06
320	$7.12846725 \times 10^{-3}$	1.03

Table 1: Numericals results for Problem 1.

6.2 Problem 2

It is a test case studied in [17]. We consider an spherical interface Σ defined by $r^2 = 1/4$ with $r = \sqrt{x^2+y^2}$. The exact solution is:

$$u(x,y) = \begin{cases} e^x \cos(y) \text{ inside } \Sigma \\ 0 \text{ otherwise,} \end{cases}$$

The numerical results and orders of convergence are presented in Table 2. We observe again a first-order convergence.

N	L^∞ error	order
20	4.9234×10^{-3}	-
40	2.2717×10^{-3}	1.12
80	1.0763×10^{-3}	1.10
160	5.5813×10^{-4}	1.05
320	2.4518×10^{-4}	1.08

Table 2: Numericals results for Problem 2.

References

[1] J. T. Beale and A. T. Layton. On the accuracy of finite difference methods for elliptic problems with interfaces. *Commun. Appl. Math. Comput. Sci.*, 1:91–119, 2006.

[2] P. Bethelsen. A decomposed immersed interface method for variable coefficient elliptic equations with non-smooth and discontinuous solutions. *J. Comput. Phys.*, 197:364–386, 2004.

[3] D. Bresch, T. Colin, E. Grenier, B. Ribba, and O. Saut. Computational modeling of solid tumor growth: the avascular stage. *SIAM J. Sci. Comput.*, 32:2321–2344, 2009.

[4] F. Buret, N. Faure, L. Nicolas, R. Perussel, and C. Poignard. Numerical studies on the effect of electric pulses on an egg-shaped cell with a spherical nucleus. Technical Report 7270, INRIA, 2010.

[5] I. Chern and Y.-C. Shu. A coupling interface method for elliptic interface problems. *J. Comput. Phys.*, 225:2138–2174, 2007.

[6] P. G. Ciarlet. Discrete maximum principle for finite-difference operators. *aequationes mathematicae*, 4:338–352, 1970.

[7] M. Cisternino and L. Weynans. A parallel second order cartesian method for elliptic interface problems. *Commun. Comput. Phys.*, 12:1562–1587, 2012.

[8] F. Gibou, R. P. Fedkiw, L.T. Cheng, and M. Kang. A second order accurate symmetric discretization of the poisson equation on irregular domains. *J. Comput. Phys.*, 176:205–227, 2002.

[9] F. Gibou and R.P. Fedkiw. A fourth order accurate discretization for the laplace and heat equations on arbitrary domains, with applications to the stefan problem. *J. Comput. Phys.*, 202:577–601, 2005.

[10] Arthur Guittet, Mathieu Lepilliez, Sebastien Tanguy, and FrÃ©dÃ©ric Gibou. Solving elliptic problems with discontinuities on irregular domains â the voronoi interface method. *Journal of Computational Physics*, 298:747 – 765, 2015.

[11] H. Huang and Z. Li. Convergence analysis of the immersed interface method. *IMA J. Numer. Anal.*, 19:583–608, 1999.

[12] O. Kavian, M. Leguebe, C. Poignard, and L. Weynans. Classical electropermeabilization modelling at the cell scale. *J. Math. Biol.*, 68:235–265, 2014.

[13] M. Leguebe, C. Poignard, and L. Weynans. A second-order cartesian method for the simulation of electropermeabilization cell models. *J. Comput. Phys.*, 292:114–140, 2015.

[14] R. J. Leveque and L.Z. Li. The immersed interface method for elliptic equations with discontinuous coefficients and singular sources. *SIAM J. Numer. Anal.*, 31(4):1019–1044, 1994.

[15] Z.L. Li. A fast iterative algorithm for elliptic interface problems. *SIAM J. Numer. Anal.*, 35:230–254, 1998.

[16] Z.L. Li and K. Ito. Maximum principle preserving schemes for interface problems with discontinuous coefficients. *SIAM J. Sci. Comput.*, 23:339–361, 2001.

[17] X.-D. Liu, R. Fedkiw, and M. Kang. A boundary condition capturing method for poisson's equation on irregular domains. *J. Comput. Phys.*, 160:151–178, 2000.

[18] Bergmann M. and Weynans L. A sharp cartesian method for incompressible flows with large density ratios. Technical Report 8926, INRIA, 2016.

[19] A. Mayo. The fast solution of poisson's and the biharmonic equations on general regions. *SIAM J. Numer. Anal.*, 21:285–299, 1984.

[20] S. Osher and R. Fedkiw. *Level Set Methods and Dynamic Implicit Surfaces*. Springer, 2003.

[21] S. Osher and J. A. Sethian. Fronts propagating with curvature-dependent speed: Algorithms based on hamilton-jacobi formulations. *J. Comput. Phys.*, 79(12), 1988.

[22] J. A. Sethian. *Level Set Methods and Fast Marching Methods*. Cambridge University Press, Cambridge, UK, 1999.

[23] J. A. Sethian. Evolution, implementation, and application of level set and fast marching methods for advancing fronts. *J. Comput. Phys.*, 169:503–555, 2001.

[24] A. Wiegmann and K. Bube. The explicit jump immersed interface method: finite difference method for pdes with piecewise smooth solutions. *SIAM J. Numer. Anal.*, 37(3):827–862, 2000.

[25] S. a Yu and G.W. Wei. Three-dimensional matched interface and boundary (mib) method for treating geometric singularities. *J. Comput. Phys.*, 227:602–632, 2007.

[26] Y. C. Zhou and G. W. Wei. On the fictitious-domain and interpolation formulations of the matched interface and boundary (mib) method. *J. Comput. Phys.*, 219:228–246, 2006.

[27] Y. C. Zhou, S. Zhao, M. Feig, and G. W. Wei. High order matched interface and boundary method for elliptic equations with discontinuous coefficients and singular sources. *J. Comput. Phys.*, 213:1–30, 2006.

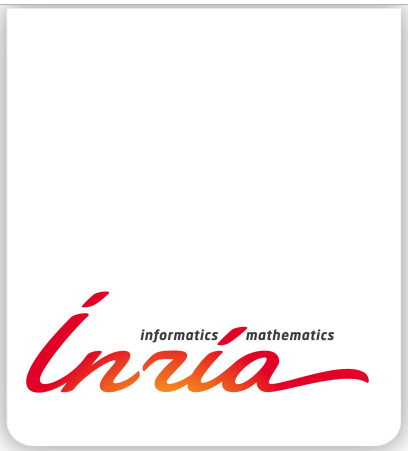

RESEARCH CENTRE
BORDEAUX – SUD-OUEST

351, Cours de la Libération
Bâtiment A 29
33405 Talence Cedex

Publisher
Inria
Domaine de Voluceau - Rocquencourt
BP 105 - 78153 Le Chesnay Cedex
inria.fr

ISSN 0249-6399